ICNMM2008-62198

ESTIMATION OF NUSSELT NUMBER IN MICROCHANNELS OF ARBITRARY CROSS-SECTION WITH CONSTANT AXIAL HEAT FLUX

Ehsan Sadeghi
Department of Mechanical Engineering
University of Victoria
ehsans@uvic.ca

Majid Bahrami
Mechatronic Systems Engineering
Simon Fraser University
mbahrami@sfu.ca

Ned Djilali
Department of Mechanical Engineering
University of Victoria
ndjilai@uvic.ca

ABSTRACT

In many practical instances such as basic design, parametric study, and optimization analysis of thermal systems, it is often very convenient to have closed form relations to obtain the trends and a reasonable estimate of the Nusselt number. However, finding exact solutions for many practical singly-connected cross-sections, such as trapezoidal microchannels, is complex.

In the present study, the square root of cross-sectional area is proposed as the characteristic length scale for Nusselt number. Using analytical solutions of rectangular, elliptical, and triangular ducts, a compact model for estimation of Nusselt number of fully-developed, laminar flow in microchannels of arbitrary cross-sections with "H1" boundary condition (constant axial wall heat flux with constant peripheral wall temperature) is developed. The proposed model is only a function of geometrical parameters of the cross-section, i.e., area, perimeter, and polar moment of inertia. The present model is verified against analytical and numerical solutions for a wide variety of cross-sections with a maximum difference on the order of *9%*.

NOMENCLATURE

A = Cross-sectional area, m^2
A_{rec} = Area of limiting rectangle of a cross-section, m^2
A_{tri} = Area of limiting triangle of a cross-section

c_1, c_2, c_3 = Coefficients used in Eq. (10)
D_h = Hydraulic diameter, m
$E(\cdot)$ = Complete elliptic integral of the second kind
h = Thermal convection coefficient, W/m^2K
I_p = Polar moment of inertia, m^4
I_p^* = Dimensionless polar moment of inertia
L = Side of a rhombic cross-section, m
$\mathcal{L}$ = Characteristic length scale, m
Nu = Nusselt number
n = Number of sides of a polygon
P = Perimeter, m
q'' = Heat flux, W/m^2
T = Temperature, K
$\bar{T}$ = Mean temperature, K
T_w = Wall temperature, K
$\bar{T}_w$ = Mean wall temperature, K
w = Velocity in z- direction, m/s
$\bar{w}$ = Mean axial velocity of the fluid , m/s

Greek symbols

α = Thermal diffusion coefficient, m^2/s
ε = Aspect ratio
θ = Dimensionless temperature
$\bar{\theta}$ = Mean dimensionless temperature
Δ_{rec} = Deviation from limiting rectangle
Δ_{tri} = Deviation from limiting triangle

1 INTRODUCTION

Micro fabrication technologies make it possible to build micro-fluidic, silicon-based microchannels of different cross-sections in micro flow devices such as micro-heat sinks, micro-biochips, micro-reactors and micro-nozzles [1, 2]. It is evident that the understanding of the micro scale transport phenomena is important for the designer of microfluidic devices. For this reason, many studies have been conducted in order to analyze the behavior of the convective flow through microchannels. Reviews of these works have been presented in [3- 6].

Using the electrochemical technique to obtain mass transfer coefficients for rectangular microchannels, Acosta et al. [7] showed that the smooth channel correlations for large-sized channels hold for smooth microchannels in laminar and turbulent regimes. Rahman and Gui [8] investigated the laminar forced convection of water in etched silicon microchannels; they found that the Nusselt numbers were higher than those predicted by analytical solutions for developing laminar flows through rectangular channels.

Shah and London [9] studied heat transfer in ducts for a wide variety of cross-sectional geometries. They reviewed existing studies and calculated Nusselt number for isothermal and isoflux wall conditions numerically.

Muzychka et al. [10] used the square root of the cross-sectional area of a channel to define the Nusselt number and showed that this length scale is more appropriate than the hydraulic diameter. They proposed two bounds for the Nusselt number of various geometries and developed correlations for these two bounds based on the Fanning friction factor of a rectangular channel.

Duncan and Peterson [4] reviewed micro scale convective, conduction and radiation heat transfer. Peng and Wang [11] reported a review of their extensive research on the one-phase and two-phase micro scale convective heat transfer. Peng et al. [12] analyzed the role of the dimensions of the rectangular microchannels on the Nusselt numbers in laminar and turbulent regimes. They found a strong dependence of the Nusselt number on the aspect ratio of the microchannel and proposed some correlations in which the empirical constants are functions of the microchannel dimensions [12]. Bailey et al. [6] concentrated their attention on the single phase forced convection through microchannels and concluded that the literature is inconclusive with respect to the effect of miniaturization on heat transfer and pressure drop. Many of these studies [4, 6, 11, 12], highlighted that, in many cases, the experimental results for laminar flow through microchannels deviate significantly from the predictions of the conventional theory.

Our literature review indicates that there is no general predictive model for the Nusselt number of an arbitrary cross-section microchannel. Also existing experimental data are inconsistent and sometimes contradictory. For instance, Jiang et al. [13] and Wu et al. [14] reported that in the laminar regime the Nusselt number increases with the Reynolds number with an exponent ranging from *0.3* to *1.96* whereas Gao et al. [15] and Qu et al. [16] showed that in the laminar regime the Nusselt number decreases when the Reynolds number increases.

Analytical, experimental, and numerical models have been developed to predict the Nusselt number in ducts since the *1960's*. Several hundred papers on Nusselt number have been published which illustrates the importance of this topic, and also indicates that the development of a general predictive model is difficult.

In the present study, a compact predictive model is proposed to estimate the Nusselt number for a wide variety of cross-section geometries of channels and microchannels. The proposed model is only a function of geometrical parameters of the cross-section, i.e., perimeter, area, and polar moment of inertia.

2 PROBLEM STATEMENT

Consider a microchannel with an arbitrary constant cross-section as shown in Fig. 1. To calculate the Nusselt number, following assumptions are made:

- Fully developed, steady-state, laminar, and continuum flow
- Incompressible flow
- Constant viscosity and thermal conductivity
- Negligible viscous dissipation
- Negligible rarefaction, slip/jump and surface effects
- Constant cross-sectional area A and constant perimeter P
- Constant axial wall heat flux with constant peripheral wall temperature ("H1" boundary condition)
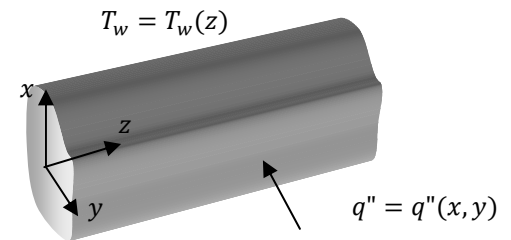

FIGURE 1. LONG MICROCHANNEL OF ARBITRARY CONSTANT CROSS-SECTION, $L \gg \sqrt{A}$.

Using the above assumptions, the energy equation reduces to [9]:

$$\nabla^2 T = \frac{w}{\alpha}\frac{\partial T}{\partial z} \quad \text{with } T = T_w(z) \text{ on the channel wall} \qquad (1)$$

where, w is the axial velocity and α is the thermal diffusion coefficient of the fluid. The energy balance can be expressed as:

$$q''.P = \dot{m}c_p\frac{\partial \bar{T}}{\partial z} \qquad (2)$$

where, q'', c_p, and $\bar{T}$ are the wall heat flux, constant pressure specific heat, and the mean temperature of z planes, respectively. $\dot{m}$ is the mass flow rate of the fluid, $\dot{m} = \rho\bar{w}A$.

Applying Eq. (2) and introducing the dimensionless parameter $\theta = (T_w - T)/(q''\mathcal{L}/k)$, the energy equation, Eq. (1), after some algebraic manipulations can be simplified to:

$$\nabla^2\theta = \left(\frac{P}{LA\bar{w}}\right)w, \text{ with } \theta = 0 \text{ on the channel wall} \qquad (3)$$

where $P, A, \mathcal{L}$ are the perimeter, the area, and an appropriate characteristic length scale, respectively. Also, $\bar{w}$ is the mean axial velocity of the fluid. The Nusselt number based on Eq. (3) can be expressed as:

$$Nu_{\mathcal{L}} = \frac{h\,\mathcal{L}}{k} = \frac{[q''/(T_w - \bar{T})]\mathcal{L}}{k} = \frac{1}{\bar{\theta}} \qquad (4)$$

where, $\bar{\theta}$ is the area-weighted average dimensionless temperature of the channel cross-section. To find the Nusselt number, $\bar{\theta}$ must be calculated by solving Eq. (3). This equation is coupled with the momentum equation. As a result, finding analytical solutions of Eq. (3) for complex geometries of microchannel cross-sections is highly unlikely.

3 CHARACTERISTIC LENGTH SCALE

To define the Nusselt number, it is conventional to use the ratio of area over perimeter $D_h = 4A/P$; i.e. the hydraulic diameter, as the characteristic length scale for non-circular channels. Figure 2 compares the analytical solutions of the "H1" Nusselt number for elliptical and rectangular ducts using hydraulic diameter and square root of cross-sectional area as characteristic length. Elliptical and rectangular cross-sections cover a wide range of singly connected microchannels and also these are two bounds of hyperellipse cross-sections, $(x/a)^n + (y/b)^n = 1$, within $2 \le n \le \infty$. Marco and Han [17] expressed "H1" Nusselt number of rectangular ducts in series form which was correlated by Shah and London [9] within $\pm 0.03\%$.

$$Nu_{D_h} = 8.235\,[1 - 2.0421\,\varepsilon + 3.0853\,\varepsilon^2 - 2.4765\,\varepsilon^3$$
$$+ 1.0578\,\varepsilon^4 - 0.1861\,\varepsilon^5] \qquad (5)$$

where, the Nusselt number is based on the hydraulic diameter of the cross-section. It can be converted to the Nusselt number based on the square root of area through:

$$Nu_{\sqrt{A}} = \frac{P}{4\sqrt{A}}\,Nu_{D_h} \qquad (6)$$

Tyagi [18] found an analytical solution for "H1" Nusselt number of elliptical ducts.

$$Nu_{\sqrt{A}} = \frac{9\pi^2}{E(1-\varepsilon^2)\sqrt{\pi\varepsilon}} \left\{ \frac{(1+\varepsilon^2)[(1+\varepsilon^4)+6\varepsilon^2]}{17(1+\varepsilon^4)+98\varepsilon^2} \right\} \qquad (7)$$

where, $E(\cdot)$ is the complete elliptic integral of the second kind. As can be seen in Fig. 2, the square root of area $\sqrt{A}$, as the characteristic length scale, leads to more consistent trends in the solutions of elliptical and rectangular ducts. These shapes cover a wide variety of cross-sections; thus, it can be concluded that the square root of area $\sqrt{A}$ is a more appropriate length scale for Nusselt number as Muzychka et al. [10] proposed. Bahrami et al. [2, 19] showed that the difference between the Poiseuille number, $fRe_{\sqrt{A}}$, of elliptical and rectangular ducts is less than 8% over a wide range of aspect ratio. Considering the analogy existing between the Poiseuille number and the Nusselt

number [20], similar trends are expected for the Nusselt numbers of these shapes. However, in spite of similar trends, the relative difference between Nusselt numbers of rectangular and elliptical channels is high and reaches up to 35% for small values of aspect ratio ($\varepsilon < 0.1$).Thus, developing a general geometric model for the Nusselt number is complicated or impossible. The goal of the present study is to develop a geometric model applicable to several cross-sections.
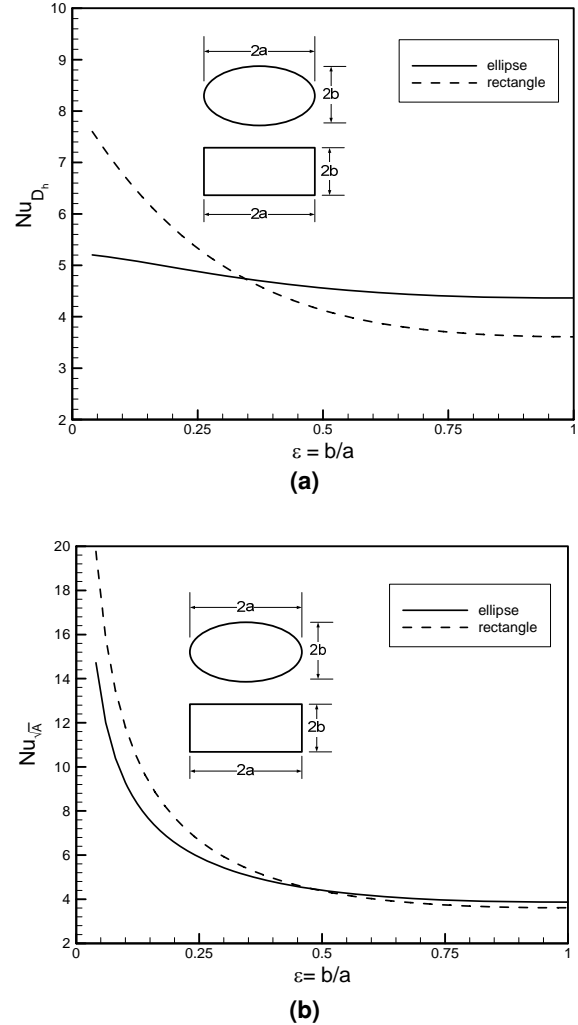

(a)

(b)

FIGURE 2. COMPARSION BETWEEN ANALYTICAL SOLUTIONS OF NU FOR ELLIPTICAL AND RECTANGULAR DUCTS USING: (a) HYDRAULIC DIAMETER AND (b) SQUARE ROOT OF AREA AS CHARACHTERSITIC LENGTH.

4 PROPOSED MODEL

Bahrami et al. [2, 19] developed a compact model for Poiseuille number, $fRe_{\sqrt{A}}$, which is only a function of geometrical parameters of the cross-section, i.e., perimeter, area, and polar moment of inertia. They started from the analytical solution of elliptical channel and established their model. It was shown that their model is applicable to a wide range of cross-sections. Considering the analogy between the Poiseuille number and the Nusselt number [20], the approach proposed by Bahrami et al. [2, 19] is followed to develop a general model for "H1" Nusselt

Copyright © 2008 by ASME

number as a function of geometrical parameters of the cross-section.

The solution of elliptical channel is selected to develop a general model, not because it is likely to occur more frequently in practice, but rather because of its unique geometrical property of its Nusselt number solution, Eq. (7). Applying the definitions of perimeter, area, and polar moment of inertia for elliptical cross-section into Eq. (7), the Nusselt number for elliptical ducts can be rewritten as:

$$Nu_{\sqrt{A}} = \left(\frac{144}{17}\,\pi^2 I_p^* \frac{\sqrt{A}}{P}\right) \underbrace{\left(\frac{I_p^{*2} + \frac{1}{4\pi^2}}{I_p^{*2} + \frac{4}{17\pi^2}}\right)}_{\approx 1} \qquad (8)$$

where, I_p^* is dimensionless polar moment of inertia about the center of the cross section, I_p/A^2. The second bracket in the right hand side of the above equation is approximately equal to unity; therefore, this equation can be simplified to:

$$Nu_{\sqrt{A}} = 8.47\,\pi^2 I_p^* \frac{\sqrt{A}}{P} \qquad (9)$$

The above equation shows that the Nusselt number can be expressed as only a function of geometrical parameters for elliptical ducts. To validate this geometrical function as a general model, the exact values of Nu for some cross-sections are compared with the geometrical function, Eq. (9). A comparison between the analytical solution of rectangular channel and the solution obtained from Eq. (9) shows that:

  i. Equation (9) agrees with analytical solution when $\varepsilon > 0.4$.
  ii. For lower aspect ratios, the difference becomes relatively high, 17.1% when $\varepsilon = 0.05$.
  iii. Moreover, when Eq. (9) is applied to other geometries such as rhombus and trapezoid, results are far from analytical or numerical solutions for some aspect ratios and convince us that Eq. (9) is not appropriate to use as a general model.
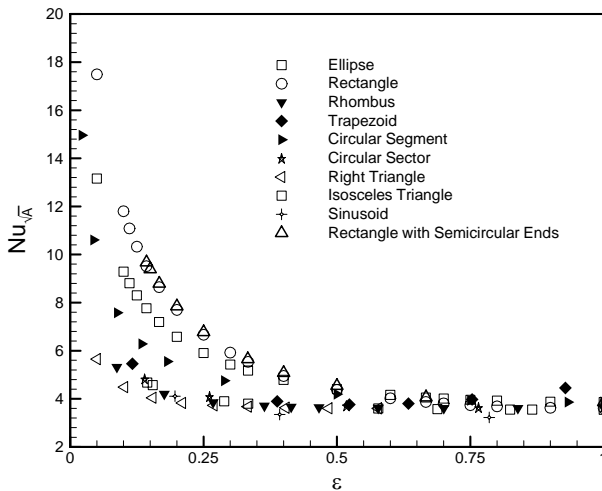

FIGURE 3. NUSSELT NUMBER FOR VAROIUS CROSS-SECTION GEOMETRIES VERSUS ASPECT RATIO.

Figure 3 shows that Nusselt numbers for different geometries are not in agreement. However, two bounds can be recognized for Nusselt numbers, where, the upper bound is provided by elliptical and rectangular cross-sections and the lower bound is presented by triangular cross-sections. Thus, different cross-sections can be categorized into three groups: 1) cross-sections close to rectangle/ellipse, 2) cross-sections close to triangle, and 3) cross-sections close to both of the previous groups.

Equation (9) shows the Nusselt number as a function of I_p^*, $\sqrt{A}/P$ for elliptical ducts. It implies that if there is a general model for various geometries, it can be a function of I_p^*, $\sqrt{A}/P$. Thus, a new model is proposed as a product function of geometric parameters of the cross-section, i.e. dimensionless polar moment of inertia I_p^*, and square root of area over perimeter $\sqrt{A}/P$.

$$Nu_{\sqrt{A}} = c_1 \left(I_p^*\right)^{c_2} \left(\frac{\sqrt{A}}{P}\right)^{c_3} \qquad (10)$$

The proposed model, Eq. (10), consists of three submodels: upper, lower, and middle. Coefficients $c_1, c_2,$ and c_3 are determined by minimizing differences between Eq. (10) and analytical solutions of elliptical and rectangular ducts for the upper model, and that of right triangular and isosceles triangular ducts for the lower model. The middle model is defined as the average of the upper and the lower models. Coefficients $c_1, c_2,$ and c_3 are listed in Table 1 for the proposed model.

TABLE 1. COEFFICIENTS OF THE PROPOSED MODEL.

Model \ Coefficient	c_1	c_2	c_3
upper	108.84	1.04	1.09
lower	7.91	0.38	0.15
middle	$\dfrac{upper\ model + lower\ model}{2}$		

To apply the model, first we should find out which submodel is appropriate to use. Relative deviation of the channel cross-sectional area from rectangular and triangular shapes is proposed as a measure to select the proper submodel. The reference rectangular and triangular cross-section is defined based on the limiting cases of geometry. These limiting cases generally occur in bounds of aspect ratios or shape angles. For instance, as shown in Table 2, the trapezoid yields rectangle when the aspect ratio goes to zero and/or ϕ goes to 90 and approaches the triangle when the aspect ratio becomes higher and the upper base goes to zero. Figure 4 illustrates the procedure to apply the model.

TABLE 2. LIMITING CASES FOR TRAPEZOIDAL CROSS-SECTION.

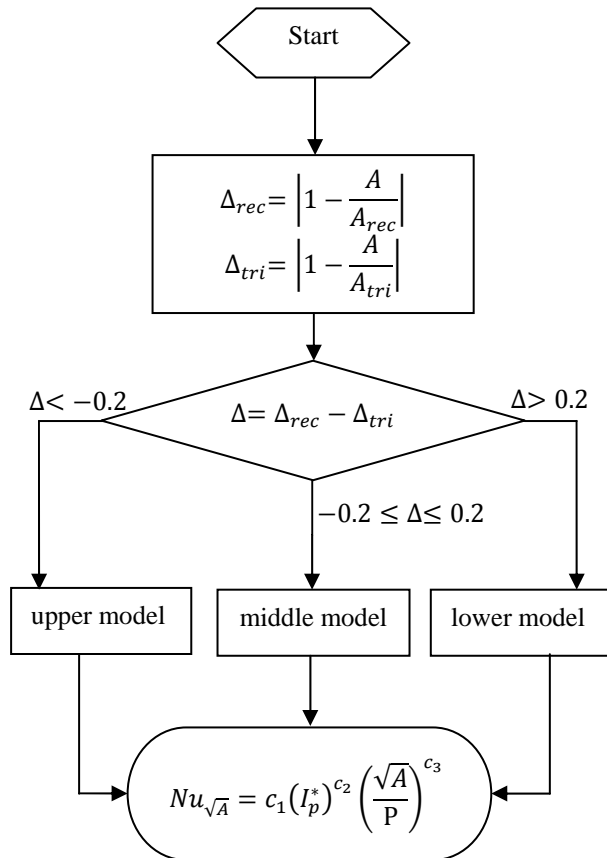| cross-section	limiting cases	appropriate submodel
		upper
		middle
		lower

FIGURE 4. FLOWCHART FOR APPLYING THE PROPOSED MODEL.

5 VALIDATION OF THE MODEL

In this section, the present model is compared with numerical results of Shah and London [9] for various cross-sections. Equation (5) is used to convert the reported Nusselt number in the literature from D_h base to $\sqrt{A}$ base. Geometrical parameters required for evaluating the Nusselt number are reported for various geometries in Table 3.

5.1 Elliptical and Rectangular Channels

Elliptical and rectangular cross-sections are bases for developing the upper model. Rectangular cross-section can be manufactured by photolithographic-based processes such as Si chemical etching and has various engineering applications [5]. Figure 5 shows the comparison between numerical results [9] and the model for elliptical and rectangular cross-sections. The difference between the present model and numerical results is less than *8%* for these shapes.
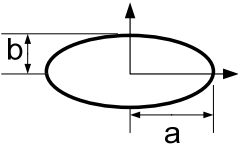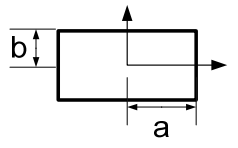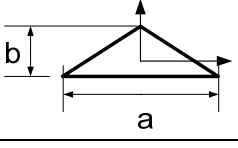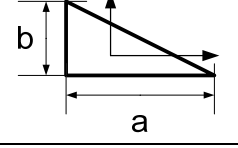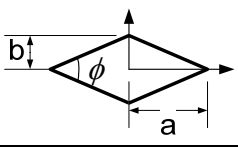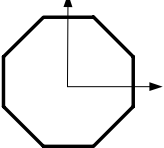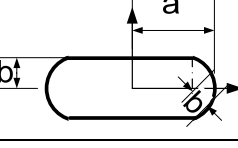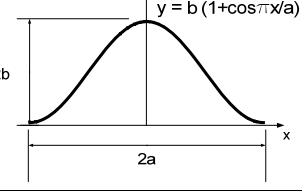

(a)

(b)
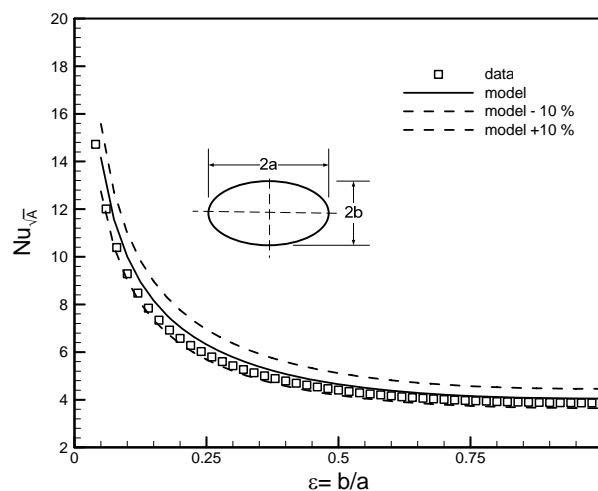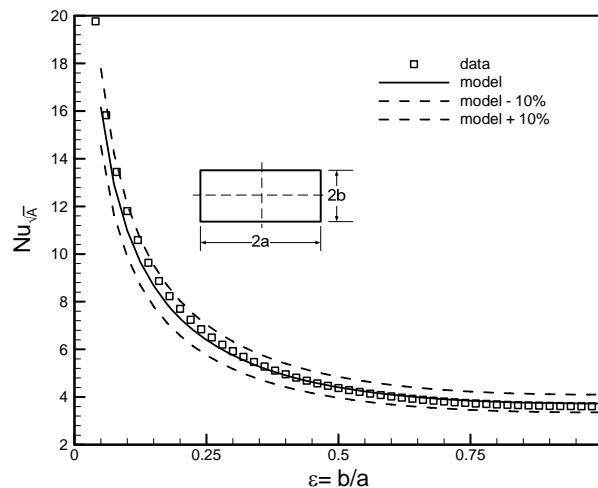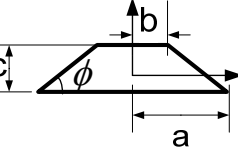
FIGURE 5. COMPARSION OF PRESENT MODEL AND NUMERICAL VALUES [9] FOR: (a) ELLIPTICAL CHANNEL, (b) RECTANGULAR CHANNEL.

5   Copyright © 2008 by ASME

TABLE 3. GEOMETRIC PARAMETERS OF STUDIED CROSS-SECTIONS.

cross-section	aspect ratio	$\sqrt{A}/P$	I_p^*
	$\varepsilon = \dfrac{b}{a}$	$\dfrac{\sqrt{\pi \varepsilon}}{4\,E(1-\varepsilon^2)}$	$\dfrac{1+\varepsilon^2}{4\pi\,\varepsilon}$
	$\varepsilon = \dfrac{b}{a}$	$\dfrac{\sqrt{\varepsilon}}{2\,(1+\varepsilon)}$	$\dfrac{1+\varepsilon^2}{12\,\varepsilon}$
	$\varepsilon = \dfrac{b}{a}$	$\dfrac{\sqrt{2\varepsilon}}{2\left(1+\dfrac{1}{\sin\phi}\right)}$	$\dfrac{\varepsilon}{9}+\dfrac{1}{12\,\varepsilon}$
	$\varepsilon = \dfrac{b}{a}$	$\dfrac{\sqrt{2\varepsilon}}{2\left(1+\varepsilon+\sqrt{1+\varepsilon^2}\right)}$	$\dfrac{1}{9}\left(\varepsilon+\dfrac{7}{9\,\varepsilon}\right)$
	$\varepsilon = \dfrac{c}{a+b}$	$\dfrac{1}{2\left(\dfrac{1}{\varepsilon}+\dfrac{1}{\sin\phi}\right)\sqrt{\varepsilon}}$	$\dfrac{2(\varepsilon^2+3)+\beta^{(1)}(\varepsilon^2-3)}{36\,\varepsilon}$
	$\varepsilon = \dfrac{b}{a}$	$\dfrac{\sqrt{\sin\phi}}{4}$	$\dfrac{1}{6\,\sin\phi}$
	$\varepsilon = 1$	$\dfrac{1}{2\,\sqrt{n\tan(\pi/n)}}$	$\dfrac{1}{6n}\left(\tan(\pi/n)+\dfrac{3}{\tan(\pi/n)}\right)$
	$\varepsilon = \dfrac{b}{a}$	$\dfrac{\sqrt{4\varepsilon\,(1-\varepsilon)+\pi\,\varepsilon^2}}{2(2-2\varepsilon+\pi\,\varepsilon)}$	$\dfrac{f^{(2)}}{(4\varepsilon\,(1-\varepsilon)+\pi\,\varepsilon^2)^2}$
	$\varepsilon = \dfrac{b}{a}$	$\dfrac{\sqrt{2\varepsilon}}{2+\dfrac{2}{\pi}\,E(-\pi^2\varepsilon^2)}$	$\dfrac{1}{12\varepsilon}\left(2-\dfrac{12}{\pi^2}+5\varepsilon^2\right)-\dfrac{9\varepsilon}{32}$

(1) $\beta = 1 - \dfrac{\varepsilon^2}{\tan\phi^2}$ (2) $f = \left[\dfrac{4\varepsilon\,(1-\varepsilon)[\varepsilon^2+(1-\varepsilon)^2]}{3} + 2\varepsilon^2\left(\dfrac{\pi}{4}-\dfrac{8}{9\pi}\right) + \pi\,\varepsilon^2\left(1-\varepsilon+\dfrac{4\varepsilon}{3\pi}\right)^2\right]$

5.2 Triangular Channels

The lower model is developed based on the solutions of different types of triangular cross-sections. Figure 6 shows the comparison between numerical results [9] and the model. The maximum difference between the present model and numerical results is *6.6%*.
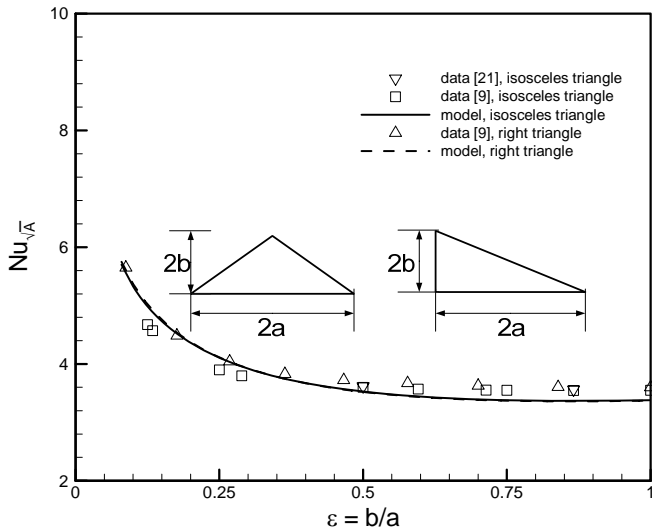

FIGURE 6. COMPARISON OF PRESENT MODEL AND NUMERICAL VALUES FOR ISOSCELES AND RIGHT ANGLE TRIANGULAR CHANNELS.

5.3 Trapezoidal Channel

Trapezoidal cross-section is an important geometry since some microchannels are manufactured with trapezoidal cross-sections as a result of the etching process in silicon wafers [5]. Furthermore, in the limit when the top side length goes to zero, it yields an isosceles triangle. At the other limit when top and bottom sides are equal, it becomes rectangle/square [2]. Figure 7 shows the comparison between the approximate model and the numerical data reported by [9] for different values of ϕ. As can be seen, except for a few points, the agreement between the model and the numerical values is reasonable (less than *8%*).
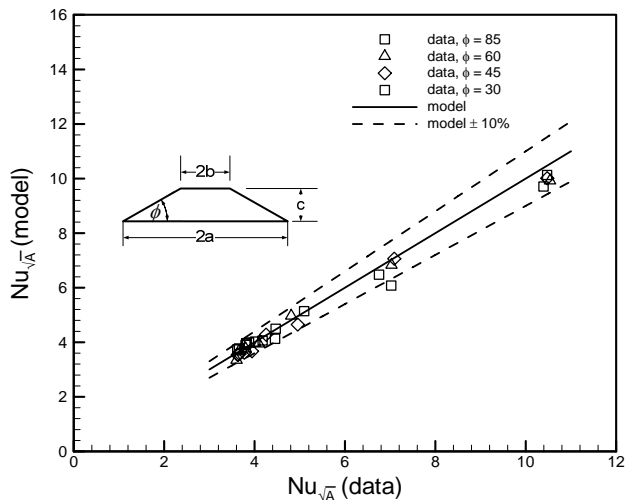

FIGURE 7. COMPARISON OF PRESENT MODEL AND NUMERICAL VALUES [9] FOR TRAPEZOIDAL CHANNEL.

5.4 Other Cross-Sections

The present model is also compared with numerical results for a number of geometries listed in Table 3. The results are shown in the following tables and figures.

TABLE 4. COMPARSION OF PRESENT MODEL AND NUMERICAL VALUES [9] FOR RHOMBIC CHANNEL.

ϕ	ε	data [9]	model	% diff.
10	0.087	5.318	5.547	4.13
20	0.176	4.201	4.511	6.87
30	0.268	3.849	4.018	4.19
40	0.364	3.703	3.721	0.49
45	0.414	3.663	3.615	-1.33
50	0.466	3.642	3.528	-3.26
60	0.577	3.618	3.398	-6.48
70	0.700	3.610	3.314	-8.93
80	0.839	3.609	3.511	-2.78
90	1	3.608	3.489	-3.41

TABLE 5. COMPARSION OF PRESENT MODEL AND NUMERICAL VALUES [9] FOR REGULAR POLYGONAL CHANNEL.

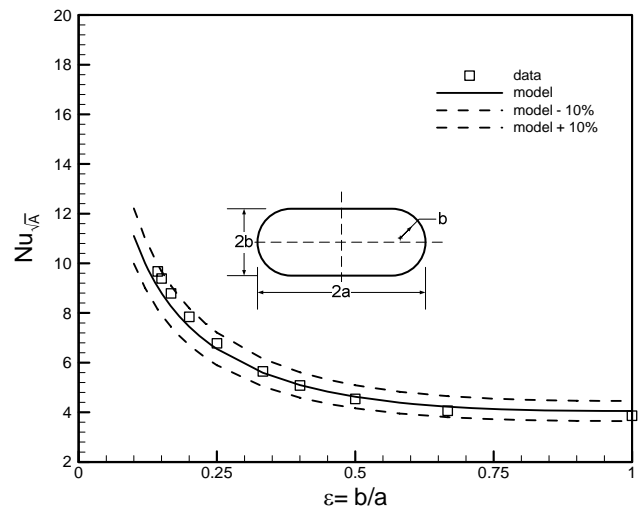| n	data [9]	model	% diff.
3	3.546	3.368	-5.27
4	3.608	3.726	3.17
5	3.678	3.809	3.46
6	3.724	3.872	3.81
7	3.766	3.915	3.81
8	3.780	3.945	4.18
9	3.797	3.966	4.26
10	3.809	3.982	4.32
20	3.852	4.033	4.49
∞	3.867	4.051	4.54

FIGURE 8. COMPARISON OF PRESENT MODEL AND NUMERICAL VALUES [9] FOR RECTANGULAR CHANNEL WITH SEMI CIRCULAR ENDS.
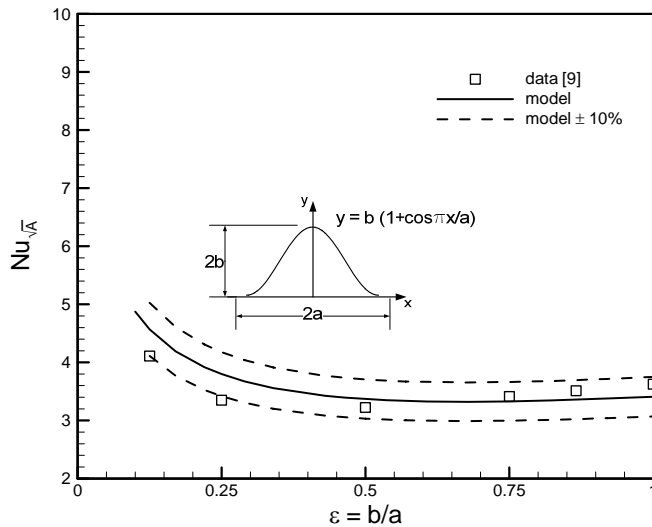
FIGURE 9. COMPARSION OF PRESENT MODEL AND NUMERICAL VALUES [9] FOR SINE CHANNEL.

6 SUMMARY AND CONCLUSIONS

In this paper, closed form relations have been developed for the Nusselt number of fully-developed laminar flow in smooth arbitrary cross-sections channels with "H1" boundary condition (constant axial wall heat flux with constant peripheral wall temperature). The square root of area $\sqrt{A}$, is adopted as the characteristic length scale, as it is superior to the conventional hydraulic diameter, D_h. Using existing analytical solutions for temperature distribution in elliptical, rectangular, and triangular ducts, a compact model including three sub models (upper, lower, and middle models) has been developed. The present model is only a function of geometrical parameters of the cross-section, i.e., area, perimeter, and polar moment of inertia. The proposed model was compared with numerical results for channels with cross-sections including: ellipse, rectangle, triangle, trapezoid, rhombus, regular polygon, rectangle with semi-circular ends, sine, and found to successfully predicts the Nusselt number for a wide variety of shapes with a maximum difference on the order of *10%*.

7 ACKNOWLEDGMENTS

8 REFERENCES

[1] Yang, C., Wu, J., Chien, H., and Lu, S., 2003, "Friction Characteristics of Water, R-134a, and Air in Small Tubes", *Microscale Thermophys. Eng.*, Vol. **7**, pp. 335–348.

[2] Bahrami, M., Yovanovich, M. M., and Culham, J. R., 2006, "Pressure Drop of Laminar, Fully Developed Flow in Microchannels of Arbitrary Cross-Section", *ASME J. of Fluid Engineering*, Vol. **126**, Sept., pp. 1036-1044.

[3] Obot, N.T., 2002, "Toward a Better Understanding of Friction and Heat/Mass Transfer in Microchannels- A Literature Review", *Journal of Nanoscale and Microscale Thermophysical Engineering*, Vol. **6**, pp. 155-173.

[4] Duncan, A.B. and Peterson, G.P., 1994, "Review of Microscale Heat Transfer", *ASME Appl. Mech. Rev.*, Vol. **47**, pp. 397–428.

[5] Morini, G.L., 2004, "Single-Phase Convective Heat Transfer in Microchannels: A Review of Experimental Results", *Int. J. Therm. Sci.*, Vol. **43**, pp. 631-651.

[6] Bailey, D.K., Ameel, T.A., Warrington, R.O., and Savoie, T.I., 1995, "Single Phase Forced Convection Heat Transfer in Microgeometries-A review", *IECEC Conference ASME-FL*, Orlando, USA, ES-396.

[7] Acosta, R.E., Muller, R.H., and Tobias, W.C., 1985, "Transport Processes in Narrow (Capillary) Channels", *AIChE J.*, Vol. **31**, pp. 473–482.

[8] Rahman, M.M. and Gui, F.J., 1993, "Experimental Measurements of Fluid Flow and Heat Transfer in Microchannel Cooling Passages in a Chip Substrate", *Advances in Electronic Packaging, ASME EEP*, Vol. **199**, pp. 685–692.

[9] Shah, R. K. and London, A. L., 1978, *Laminar Flow Forced Convection In Ducts*, Academic, New York.

[10] Muzychka, Y.S. and Yovanovich, M.M., 2002, "Laminar Flow Friction and Heat Transfer in Non-Circular Ducts and Channels: Part II - Thermal Problem", *Proceedings of Compact Heat Exchangers, A Festschrift on the 60thBirthday of Ramesh K. Shah*, Grenoble, France, pp. 131-139.

[11] Peng, X.F. and Wang, B.X., 1998, "Forced Convection and Boiling Characteristics in Microchannels", *Proceedings of 11th Int. Heat Transfer Conference*, Kyongyu, Korea, Vol. **1,** pp. 371–390.

[12] Peng, X.F., Peterson, G.P., and Wang, B.X., 1995, "Frictional Flow Characteristics of Water Flowing Through Rectangular Microchannels", *J. Exp. Heat Transfer*, Vol. **7**, pp. 249–264.

[13] Jiang, P.X., Fan, M.H., Si, G.S., and Ren, Z.P., 2001, "Thermal-Hydraulic Performance of Small Scale Micro-Channel and Porous-Media Heat Exchangers, *Int. J. Heat Mass Transfer*, Vol. **44**, pp. 1039–1051.

[14] Wu, H.Y. and Cheng, P., 2003, "An Experimental Study of Convective Heat Transfer in Silicon Microchannels with Different Surface Conditions", *Int. J. Heat Mass Transfer*, Vol. **46**, pp. 2547–2556.

[15] Gao, P., Le Person, S., and Favre-Marinet, M., 2002, "Scale Effects on Hydrodynamics and Heat Transfer in Two-Dimensional Mini and Microchannels, *Int. J. Thermal Sci.*, Vol. **41**, pp.1017–1027.

[16] Qu, W., Mala, G.M., and Li, D., 2000, "Heat Transfer for Water Flow in Trapezoidal Silicon Microchannels", *Int. J. Heat Mass Transfer*, Vol. **43**, pp. 3925–3936.

[17] Marco, S.M. and Han, L.S., 1955, "A Note on Limiting Laminar Nusselt Number in Ducts with Constant Temperature Gradient by Analogy to Thin-Plate Theory", *Trans. ASME*, Vol. **77**, pp. 625-630.

[18] Tyagi, V.P., 1966, "Laminar Forced Convection of a Dissipative Fluid in a Channel", *J. Heat Transfer*, Vol. **88**, pp. 161-169.

[19] Bahrami, M., Yovanovich, M. M., and Culham, J. R., 2007, "A Novel Solution for Pressure Drop in Singly Connected Microchannels of Arbitrary Cross-Section", *Int. J. Heat Mass Transfer*, Vol. **50**, pp. 2492-2502.

[20] Incropera, F. P. and DeWitt, D. P., 1996, *Fundamentals of Heat and Mass Transfer*, John Willey & Sons, New York.

[21] Chen, S., Chan, T.L., Leung, C.W., Yu, B., 2000, "Numerical Prediction of Laminar Forced Convection in Triangular Ducts with Unstructured Triangular Grid Method", *Journal of Numerical Heat Transfer*, Vol. **38**, pp. 209-224.